BNL-105178-2014-TECH

Booster Technical Note No. 134;BNL-105178-2014-IR

LONGITUDINAL HIGHER ORDER MODES OF THE BOOSTER PROTON RF CAVITY LOADED WITH DISPERSIVE FERRITE - SUPERFISH CALCULATION

F. Z. Khiari

December 1988

Collider Accelerator Department

Brookhaven National Laboratory

U.S. Department of Energy

USDOE Office of Science (SC)

LONGITUDINAL HIGHER ORDER MODES OF THE BOOSTER PROTON RF CAVITY LOADED WITH DISPERSIVE FERRITE - SUPERFISH CALCULATION

AD
BOOSTER TECHNICAL NOTE
NO. 134

F. KHIARI, A. LUCCIO and A. RATTI

DECEMBER 30, 1988

ACCELERATOR DEVELOPMENT DEPARTMENT
BROOKHAVEN NATIONAL LABORATORY
UPTON, NEW YORK 11973

Longitudinal Higher Order Modes of the Booster Proton RF Cavity Loaded with Dispersive Ferrite—Superfish Calculation

F. Z. Khiari, A. U. Luccio, A. Ratti

Brookhaven National Laboratory

Upton, NY 11973

INTRODUCTION

The AGS Booster is a fast cycling accelerator designed to accelerate high intensity beams of protons and heavy ions and inject them into the AGS. In the presence of high intensity beams, special care must be taken to minimize the various impedances that the beam sees when it circulates in the accelerator ring. The adverse effects of some impedances might not be seen in the Booster itself, but are nevertheless important enough to affect the beam quality in the long term so as to degrade its quality at later stages of the acceleration process. This is for example the case of longitudinal coupled-bunch instabilities. These instabilities are induced by high Q impedances, such as those of the resonant higher order modes of an accelerating cavity. These impedances are usually approximated by the frequency dependent impedance of an equivalent parallel RLC circuit, i.e.

$$Z^R(\omega) = \frac{R_{sh}}{1 + jQ(\omega/\omega_R - \omega_R/\omega)}, \tag{1}$$

where R_{sh} $[\Omega]$ and Q are the longitudinal shunt impedance and quality factor of the rf cavity at the resonant frequency ω_R. The strength of the interaction of the beam with a given higher order cavity mode and the extent to which this mode will cause a problem depends then on the quality factor and the shunt impedance of that mode. In this note we present the results of Superfish[1] calculations to find the frequencies of some of these higher order modes as well as their Qs and R_{sh}s, stating the conditions for which these calculations were made.

RESULTS OF SUPERFISH

In the proton mode of operation, the Booster will use 2 rf stations, each with 2 cylindrical resonant cavities, with a total peak voltage of 90 kV. Each cavity is 1.2 m long and has a diameter ($2R_2$) of 54 cm. The beam pipe diameter is 15 cm. In addition to the ceramic around the 4 cm wide gap and the outer capacitors in parallel with it, each cavity is loaded with 28 Philips type 4M2 ferrite rings with an inside diameter ($2r_1$) of 25 cm, an outside diameter ($2r_1$) of 50 cm, and a thickness of about 2.5 cm. The cavity also has $\approx$ 1 cm thick copper cooling plates interspaced between the ferrite rings to take some the dissipated heat away. The presence of the outer capacitors is taken into account by giving the ceramic around the gap an effectively higher dielectric constant adjusted, along with the magnetic permeability of the ferrite, to give a resonante frequency in the 2.5–4.1 MHz range of operation. A schematic of a quarter of the cavity is shown in Fig. 1. This figure also represents the region where Superfish solves Helmholtz equation

$$(\nabla^2 + k^2)\psi = 0, \tag{2}$$

where ψ is the E or H component of the electromagnetic field subject to the appropriate boundary conditions. The resonant (angular) frequency, ω_R, of each mode is related to the eigenvalue k of that mode by

$$\omega_R = \frac{k}{\sqrt{\epsilon\mu}}, \tag{3}$$

where ϵ and μ are the electric permittivity and magnetic permeability of the ferrite. Superfish uses μ of the ferrite cavity as input and solves Eqs. 2 and 3 for the resonant frequency. If μ were constant, this resonant frequency would be the one we are looking for. The problem arises for the case of a dispersive ferrite where μ is now frequency dependent. The ferrite magnetic permeability, μ, is determined by the requirements of the fundamental mode. The higher order modes, however, might occur at frequencies for which μ used in Superfish is different from the actual one and, therefore, these frequencies are not the ones we want. To find the real resonant frequencies of the higher order modes, we need to know the curve of $\mu(\omega)$ for the ferrite we are using. Such a curve is not readily available and we had to rely on the general litterature[2]. Fig. 2 shows the results of measurements on a ferrite of the NiZn type, with a NiO:ZnO ratio of 31.7:16.5, which corresponds to the ferrite (when it is biased) used in the Booster rf cavities[3]. The plot in Fig. 2 was made for the case of an unbiased ferrite. The magnetic losses in the ferrite are due to μ'', the imaginary part of μ. With k real in Eq. 3, we see that ω_R is also complex with a real part

$$\omega_R' = \frac{k}{\sqrt{\epsilon(\mu'^2 + \mu''^2)^{1/2}}} cos \frac{tan^{-1}(\mu''/\mu')}{2} \tag{4}$$

corresponding to oscillations in time, and an imaginary part

$$\omega_R'' = \frac{k}{\sqrt{\epsilon(\mu'^2 + \mu''^2)^{1/2}}} sin \frac{tan^{-1}(\mu''/\mu')}{2} \tag{5}$$

corresponding to damping due to power dissipation in the ferrite. The effective μ (μ_{eff}) used to find the resonant frequency is therefore

$$\mu_{eff} = \frac{\sqrt{(\mu'^2 + \mu''^2)}}{cos^2(\frac{tan^{-1}(\mu''/\mu')}{2})} \tag{6}$$

It is approximately constant up to about 20 MHz and changes therefrom with frequency (see Fig. 3). Therefore, the cavity modes with frequencies less than 20 MHz can exist in the cavity as they are, but the ones with frenquencies higher than 20 MHz have to be searched for individually until μ used in Superfish to find each one of them corresponds to the effective μ at the mode's eigenfrequency. One way to do this last search is to look for the intersection point of the curve of μ_{eff} versus frequency for the ferrite on the one hand, and the curve of eigenfrequency versus μ for a given mode using Superfish on the other hand. This is illustratded in Fig. 3a for some higher order modes at the beginning of the

Booster cycle. For example, with an initial μ of 100, the 2^{nd} higher order mode occurs at 45.5 MHz. But, as seen in Fig. 3a, μ_{eff} of the ferrite $\approx 88\mu_\circ$ at 45.5 MHz. We therefore did a few iterations by changing μ in Superfish until we found the intersection point. This 2^{nd} higher mode is thus shifted from 45.5 MHz to 48.8 MHz where the corresponding $\mu_{eff} = \mu = 87\mu_\circ$.

To achieve the 2.5–4.1 MHz frequency swing during acceleration, a d.c bias field is used to tune the magnetic permeability of the ferrite[5]. Data showing the variation of $\mu(\omega)$ with d.c bias field in the frequency range of the caviy higher order modes are not readily available. To evaluate the parameters of the higher order modes at later parts of the Booster cycle, when the bias field is high, we make the assumption that the d.c bias field does not affect the frequency dependence of μ' and μ'' but only affects their relative values, i.e. the curves shown in Fig. 2 are shifted downward as the bias field is increased. It is the a simple matter to find the higher order modes of the rf cavity at later stages of the acceleration cycle by applying the same technique we used for the beginning of the cycle. The results for the first two higher order modes are shown in Figs. 3b and 3c at the middle and the end of the cycle respectively. We should also note that the electric permittivities of the ferrite ($\epsilon = 32\epsilon_\circ$), the ceramic[9] ($\epsilon = 71\epsilon_\circ$), and copper ($\epsilon = \epsilon_\circ$) are kept constant during the acceleration process. It is also found that the resonant frequencies are not very sensitive to the dielectric constant of the ferrite. Figures 4a–4h show plots of the field lines for the fundamental and some of the higher order modes.

The higher order modes found are actually too numerous to list and we studied only some of them. However, if we interpolate the values of μ' and μ'' in Fig. 2 up to 1 GHz (the pipe cutoff frequency), we see that there are no high Q longitudinal ferrite modes that will affect the beam.

Beside finding the normal modes of the cavity, Superfish also calculates the quality factor, Q, and the shunt impedance, R_{sh}, of each mode. Q and R_{sh} are given by :

$$Q = 2\pi f U / \wp, \tag{7}$$

and

$$R_{sh} = E_\circ^2 L^2 / \wp, \tag{8}$$

where $f \equiv \omega/2\pi$ is the resonante frequency, U is the stored energy in the cavity, $\wp$ represents the power losses in the cavity, L is the cavity length , and

$$E_\circ = \frac{1}{L} \int_{-L/2}^{L/2} E_z(z, r = 0) dz \tag{9}$$

is the average accelerating electric field along the cavity axis. For a gap voltage of 22.5 kV ($E_\circ$ = 18.75 kV/m), f, Q, and R_{sh} of the fundamental and some of the higher order modes are listed in Table 1. The shunt impedances listed in Table 1 correspond to one cavity only. They should be multiplied by 4 to account for the existence of 4 cavities in the Booster ring.

In the previous calculations, the only losses taken into account were those in the cavity walls. Superfish does not have the option to calculate the losses in the ferrite. When these losses are taken into consideration, the Qs and R_{sh}s will be much lower. To estimate these losses, we use Fig. 2 (and the corresponding ones at later parts of the cycle) to find μ'' corresponding to a given mode eigenfrequency. The loss angle δ is related to the quality factor Q by:

$$tan\delta = \frac{\mu''}{\mu'} = \frac{1}{Q}. \tag{10}$$

This allows us to find Q, i.e.

$$Q = \frac{\mu'}{\mu''}, \tag{11}$$

The magnetic losses in the ferrite are given by[4]:

$$\wp_m = \frac{1}{2}\int\int\int \omega\mu''|H|^2 d\tau, \tag{12}$$

where H is the peak amplitude of the magnetic field and the integral is over the volume of the ferrite. $\wp_m$ can also be written as

$$\wp_m = \pi f \mu'' V < |H|^2 >_F, \tag{13}$$

where V is the volume of the ferrite and $< |H|^2 >_F \equiv (1/V)\int\int\int |H|^2 d\tau$. Assuming a $1/r$ variation for H (this assumption is good for the first few higher order modes only), $H(r)$ can be expressed in terms of H_W, the magnetic field at the cavity wall by

$$H(r) = H_W \times \frac{R_2}{r}. \tag{14}$$

where R_2 is the radius of the cavity. With $d\tau = 2\pi r dr dz$ and $V = \pi(r_2^2 - r_1^2)L_F$, where L_F is the total length of the ferrite, we get

$$< |H|^2 >_F = < |H|^2 >_W \times \frac{2R_2^2 \times \ell n(r_2/r_1)}{r_2^2 - r_1^2} \approx 2.2 \times < |H|^2 >_W, \tag{15}$$

where $< |H|^2 >_W \equiv (1/L_F)\int\int\int |H|^2(R_2, z)dz$. The power dissipation due to magnetic losses is therefore

$$\wp_m \approx 2.2\pi f \mu'' V < |H|^2 >_W . \tag{16}$$

The volume of the ferrite in each cavity $\approx .103$ m^3. Using Eq. (16) one can find the total magnetic losses in the ferrite and substitute for that in Eq. (8) to find the shunt impedance of a given mode. This is done for the fundamental and some of the higher order modes and the results are shown in Table 2. The magnetic losses predominate and are the only ones taken into account. Here also the shunt impedances should be multiplied by 4 to find the total shunt impedance of the 4 cavities.

CONCLUSIONS

We calculated the frequencies of the fundamental and some of the higer order modes of the Booster proton rf cavities and found approximate values of their shunt impedances and quality factors. Our values of Q and R_{sh} for the fundamental mode, at the beginning of the cycle, are in good agreement with the measured values on a sample ferrite ring with a very low bias field[6]. At the middle and end of the cycle, when the bias field is sizable, our values of Q and R_{sh} for the fundamental mode are comparable to the measured ones[6].

Recently, some frequency measurements have been made on a prototype Booster proton rf cavity. It was found that the fundamental mode occurs at 1.9 MHz when the total gap capacitance is about 400 pF[7]. An approximate evaluation of the capacitance of the ceramic around the gap in our case gives 369 pF. The frequency found from Superfish is 2.54 MHz. Assuming that the ferrite magnetic permeability used in the measurement is the same as the one used in Superfish, and with a $1/\sqrt{capacitance}$ variation for the frequency, we find

$$\frac{f_R^S/f_R^m}{\sqrt{C^m/C^S}} \approx 1.3, \tag{17}$$

where the superscript m (S) denotes quantities related to the measurement (Superfish).

Let us now briefly consider the effect of the impedances of the higher order modes on the beam. In a previous simulation[8], it was found that the effect on the rf capture of a broad band wall impedance of 200 Ω was negligibly small compared to the effect of the space charge impedance. From Table 2, we see that the maximum (total) R_{sh} encountered by the beam in one turn is about 4 Ω. We, therefore, expect the single bunch effects of the parasitic higher order modes to be negligible compared to the space charge effects. We recall that $|Z^{sc}/n| \approx 700\ \Omega$ at injection, and $|Z^{sc}/n| \approx 100\ \Omega$ at extraction (sc stands for space charge). To estimate the coupled bunch effects of the rf parasitic modes, we use Eqs. (4) and (5) to calculate the time (τ_e) it takes the amplitude of a given higher order mode to decrease to 1/e of its initial value and compare it to the time ($\tau_b = T_\circ/3$, $T_\circ =$

revolution period) between the centers of two consecutive proton bunches in the Booster ring. The fields are damped in the ferrite as $exp(-\omega''_R t)$. The time in question therefore is

$$\tau_e = \frac{1}{\omega''_R} = \frac{1}{\omega'_R \times (\sqrt{1+Q^2} - Q)}, \tag{18}$$

where ω'_R and Q are respectively the angular resonant frequency and quality factor of the parasitic mode. When $Q^2 >> 1$, Eq. (18) reduces to

$$\tau_e \approx \frac{2Q}{\omega'_R}. \tag{19}$$

Table 3 compares τ_e and τ_b for the parasitic higher order modes at the beginning, middle, and end of the cycle. From the table we conclude that $\tau_e << \tau_b$ at all times. The fields induced in the cavity by a given proton bunch die out before the next bunch comes along. We therefore do not expect the higher order modes found in this note to induce logitudinal coupled bunch instabilities.

ACKNOWLEDGEMENTS

We have benefitted from discusions with a number of people. We are especially grateful to Prof. Gatti for useful comments and to Michael Goldman for useful discussions and for providing us with the results of his measurements on a sample ferrite ring.

REFERENCES

[1] K. Halbach & R. F. Holsinger, Superfish—A Computer Program for Evaluation of RF Cavities with Cylindrical Symmetry, *Particle Accelerators*, **7**, 213 (1976).

[2] E.P. Wohlfarth Ed., *Ferromagnetic Materials*, Vol. No. 2, pp. 192, North-Holland (1980).

[3] M. Goldman, Private Communication.

[4] R. F. Harrington, *Time-Harmonic Electromagnetic Fields*, McGraw-Hill Book Compagny, pp. 178 (1961).

[5] R. Sanders & al, The AGS Booster High Frequency System, *BNL-41463.*

[6] J. Zhang, Calculation of the Booster Proton Cavity using the Superfish Program, *Booster Tech. Note No. 109* (1988).

[7] A. Ratti, Private Communication.

[8] F.Z. Khiari & A.U. Luccio, Effect of a Wall Impedance on the RF Capture of a Chopped Beam in the AGS Booster, *Booster Tech. Note No. 128* (1988).

[9] Technical data sheet AX-3000, Duramic Alumina, Duramic Products, Inc.

$f'_R[MHz]$	$R_{sh}[\Omega]$	Q
2.5*	37×10^6	119×10^3
26.5	181×10^3	415×10^3
48.8	49×10^3	870×10^3
63.2	32×10^3	1698×10^3
73.1	26×10^3	2626×10^3
81.4	22×10^3	3107×10^3
309.8	30×10^3	2623×10^3
724.6	89	230×10^3
3.1◇	22×10^6	88×10^3
32.9	110×10^3	299×10^3
61.7	29×10^3	606×10^3
4.1†	11×10^6	59×10^3
45.9	49×10^3	179×10^3
84.2	15×10^3	372×10^3

Table 1 Superfish output for the fundamental and some of the higher order modes in the case of no ferrite losses

* $\mu/\mu_\circ = 100$ (beginning of cycle)

◇ $\mu/\mu_\circ = 66$ (middle of cycle)

† $\mu/\mu_\circ = 38$ (end of cycle)

$f'_R[MHz]$	$\mu'/\mu_\circ$	$\mu''/\mu_\circ$	$R_{sh}[\Omega]$	Q
2.5	100	1.6	$(19/20^*)\times10^3$	$61/55^*$
26.5	100	24.7	1	4
48.8	64	44.4	0.09	1.4
63.2	48.4	50	0.04	1
73.1	43.5	50	0.04	0.9
81.4	39.3	49.7	0.02	0.8
309.8	12.1	24.5	0.02	0.5
724.6	4.6	13.5	5×10^{-6}	0.3
3.1	66	1.2	$(14/18^*)\times10^3$	$56/69^*$
32.9	61.2	21.7	0.6	2.8
61.7	32.4	33	0.06	1
4.1	38	0.78	$(9.5/12.4^*)\times10^3$	$49/55^*$
45.9	25.7	16.3	0.3	1.6
84.2	14.4	18.6	0.05	0.8

Table 2 Calculation of R_{sh} and Q for the case of ferrite losses

* Numbers from measurements[6]

$f'_R[MHz]$	$\tau_b[\mu sec]$	$\tau_e[\mu sec]$
26.5	0.4	0.05
48.8	0.4	0.01
63.2	0.4	0.006
73.1	0.4	0.005
81.4	0.4	0.004
309.8	0.4	0.0008
724.6	0.4	0.0003
32.9	0.32	0.03
61.7	0.32	0.006
45.9	0.24	0.01
84.2	0.24	0.004

Table 3 Comparison of τ_b and τ_e for some of the higher order modes at the beginning, middle, and end of the Booster cycle

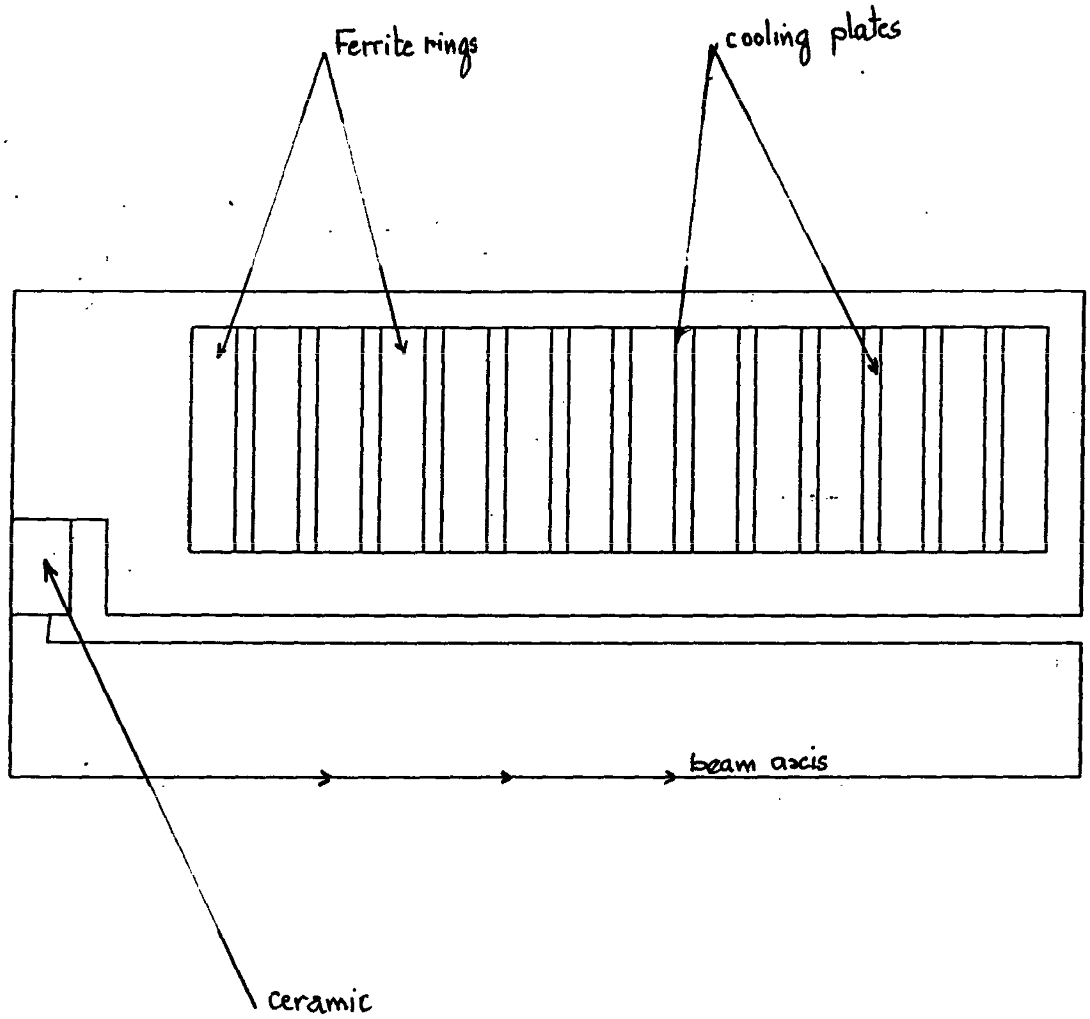

Fig. 1 Schematic of a quarter of the Booster rf cavity

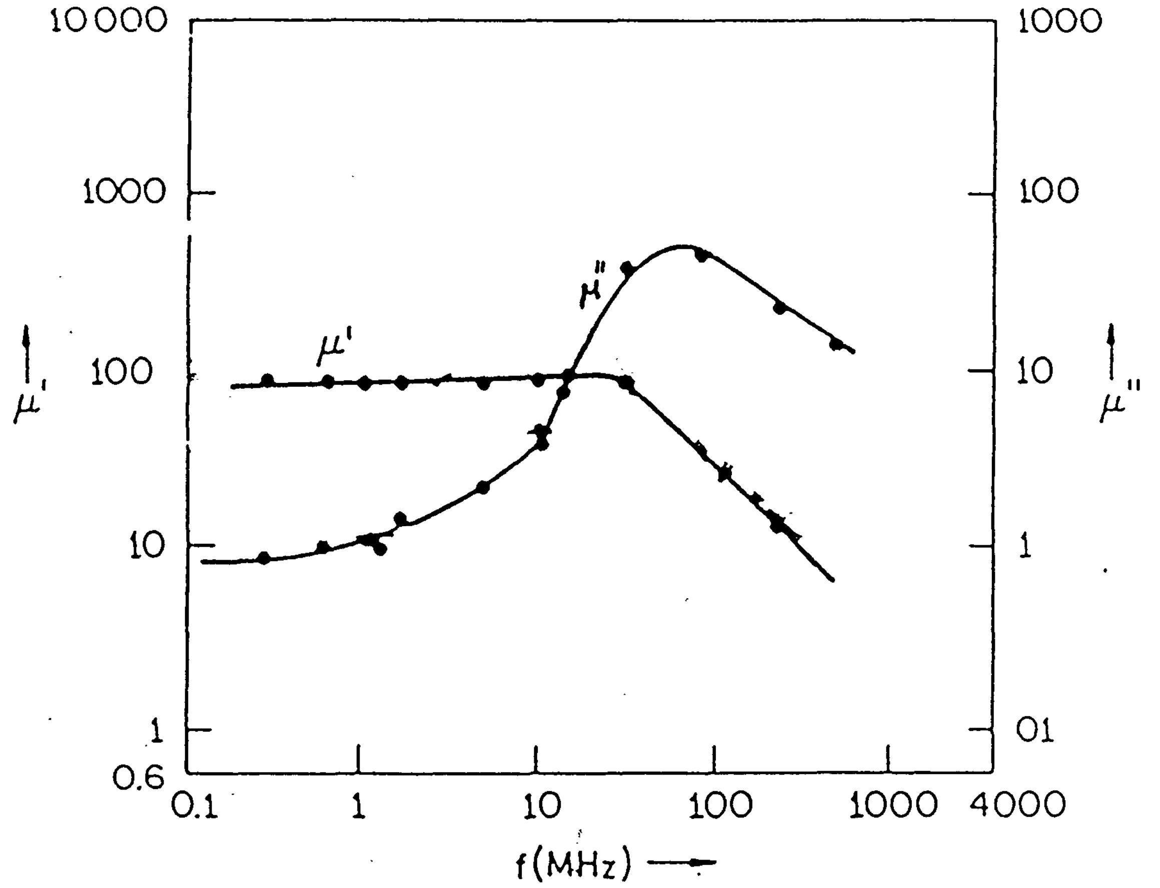

Fig. 2 Permeability spectrum for unbiased NiZn ferrite

(ratio NiO:ZnO=31.7:16.5)

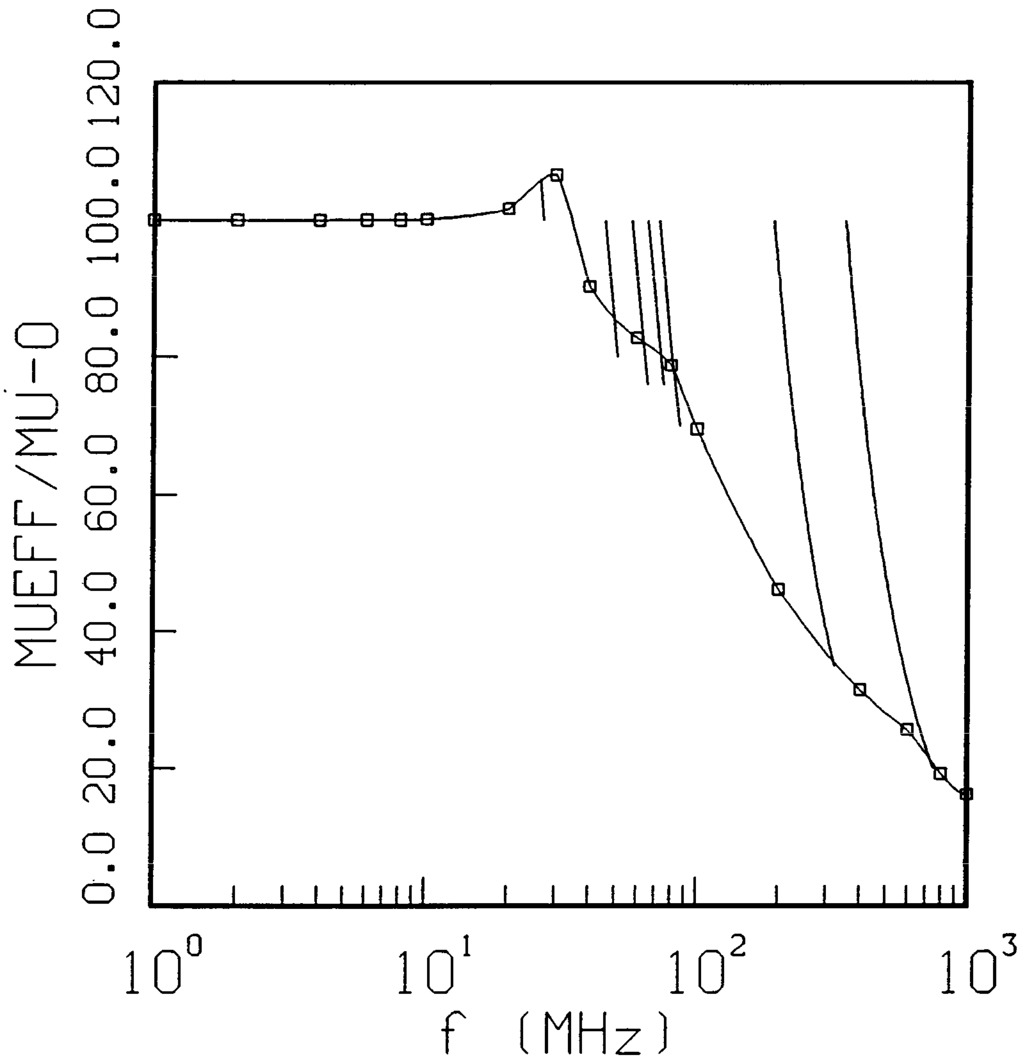

Fig. 3a Determination of f_R and μ for some of the higher order modes

(Beginning of cycle)

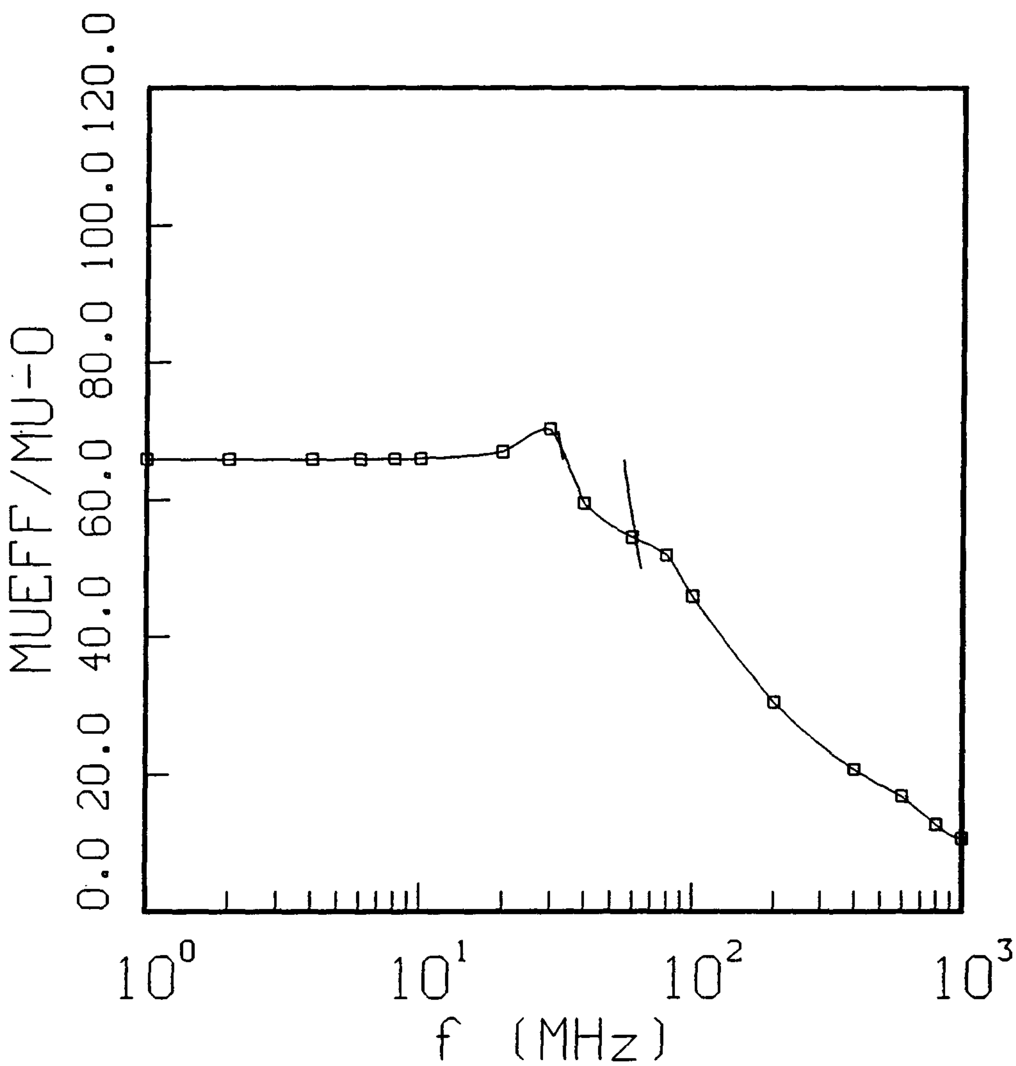

Fig. 3b Determination of f_R and μ for the first two higher order modes

(middle of cycle)

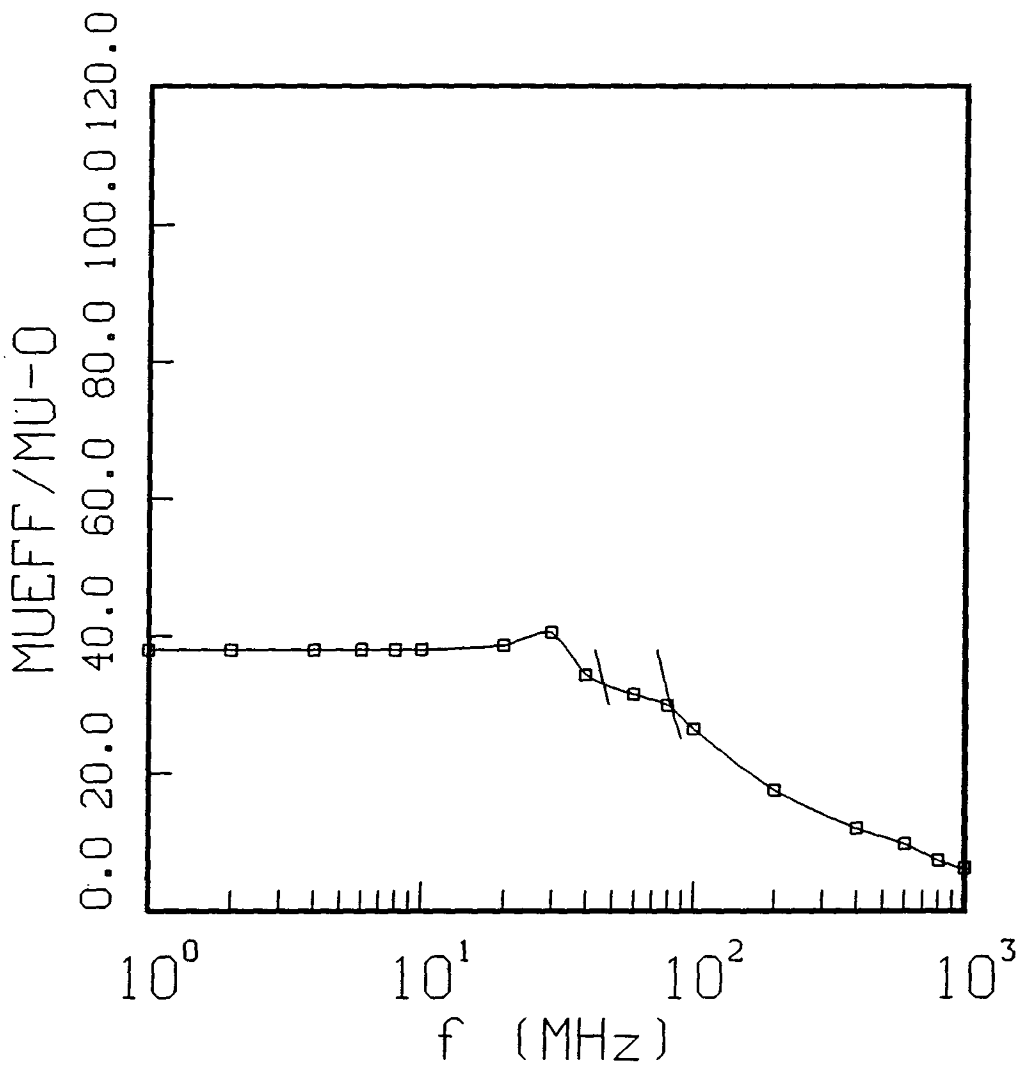

Fig. 3c Determination of f_R and μ for the first 2 higher order modes

(end of cycle)

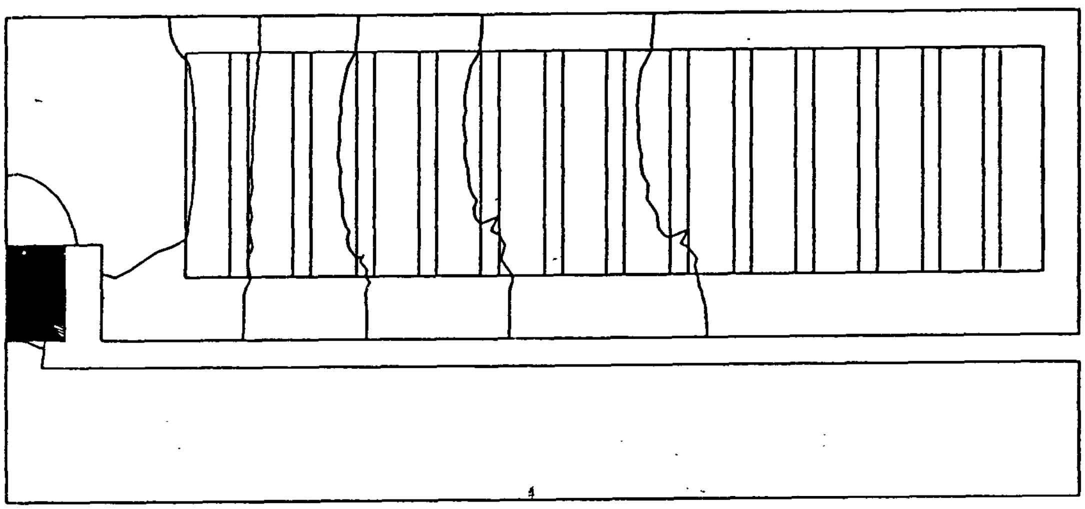

Fig. 4a Field lines of the fundamental mode, $f_R = 2.5$ MHz

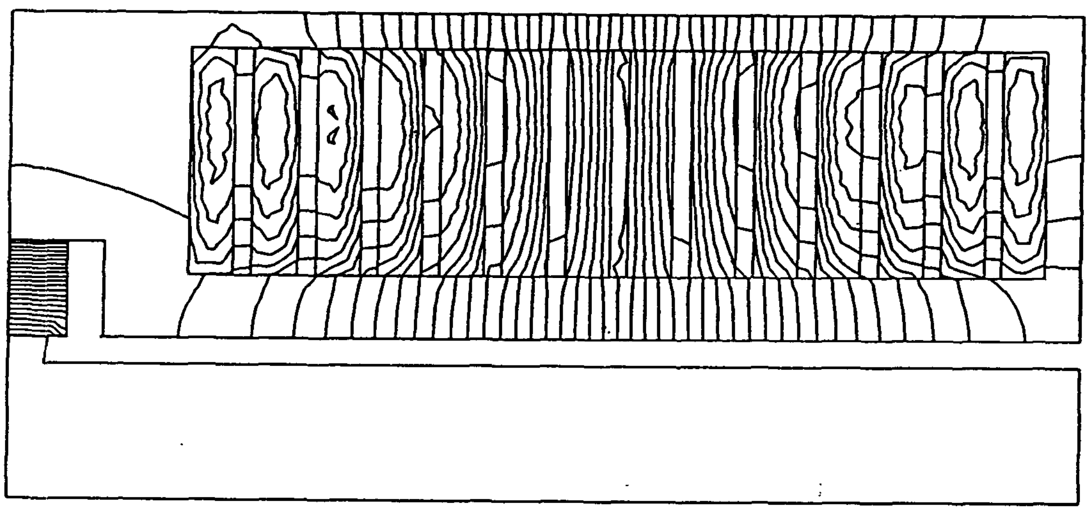

Fig. 4b Field lines of the first higher order mode, $f_R = 26.5$ MHz

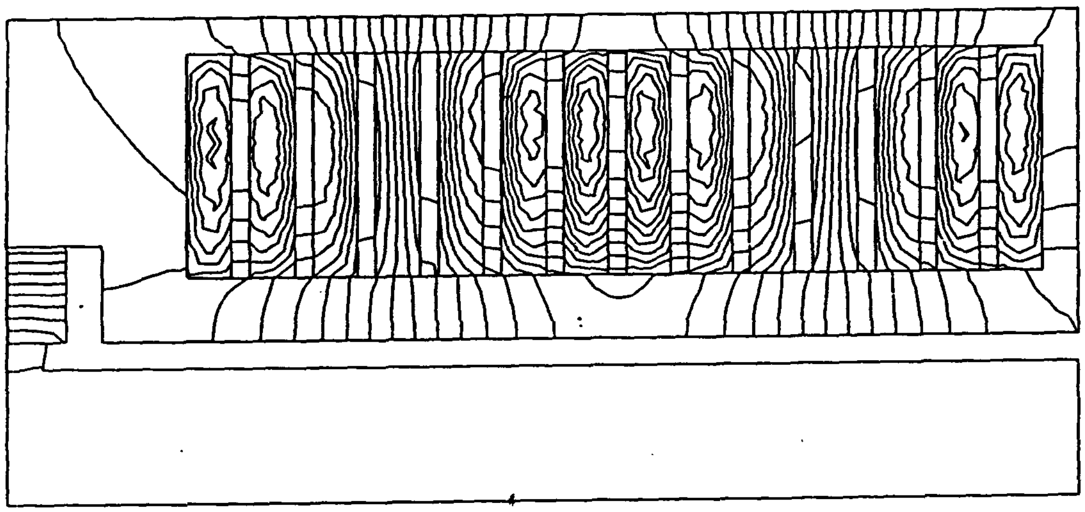

Fig. 4c Field lines of the second higher order mode, $f_R = 48.8$ MHz

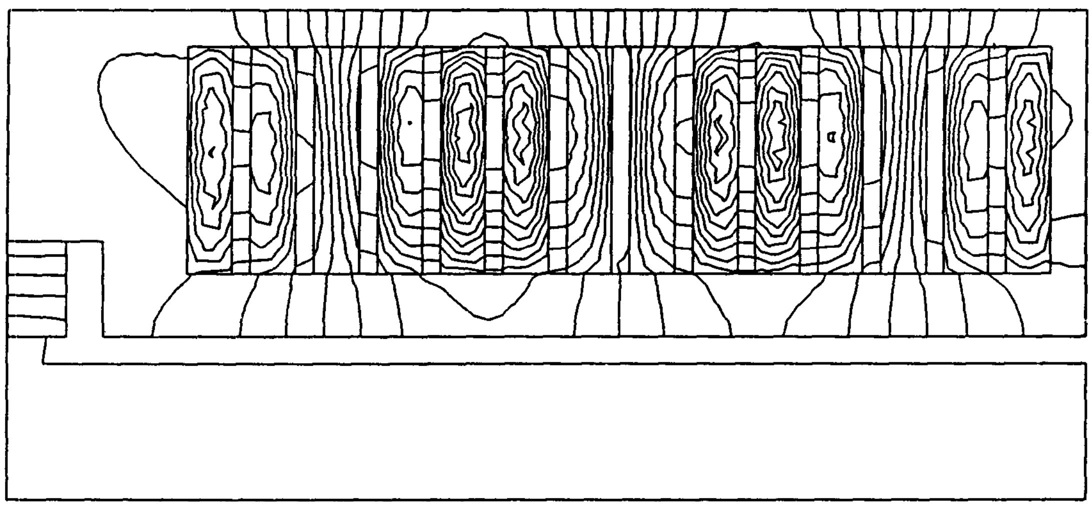

Fig. 4d Field lines of the third higher order mode, $f_R = 63.2$ **MHz**

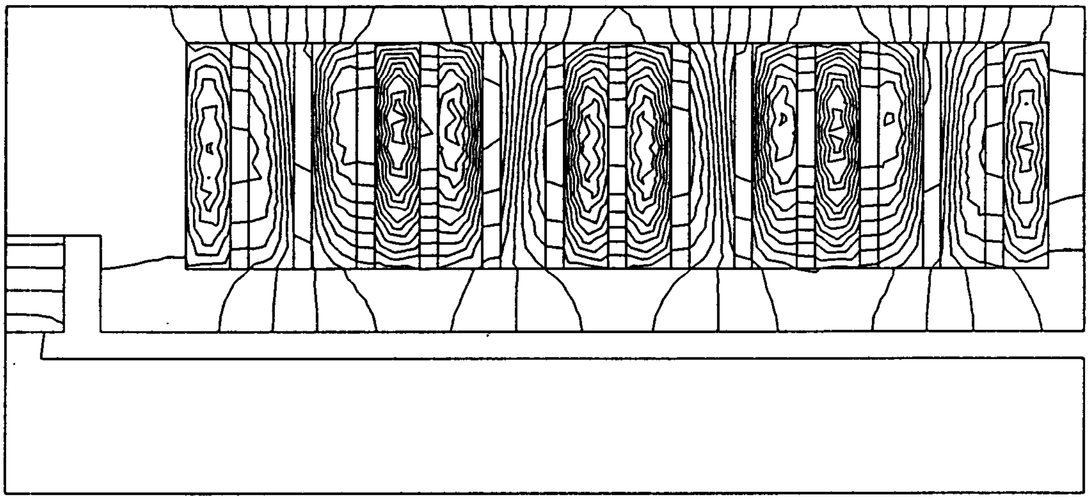

Fig. 4e Field lines of the fourth higher order mode, $f_R = 73.1$ MHz

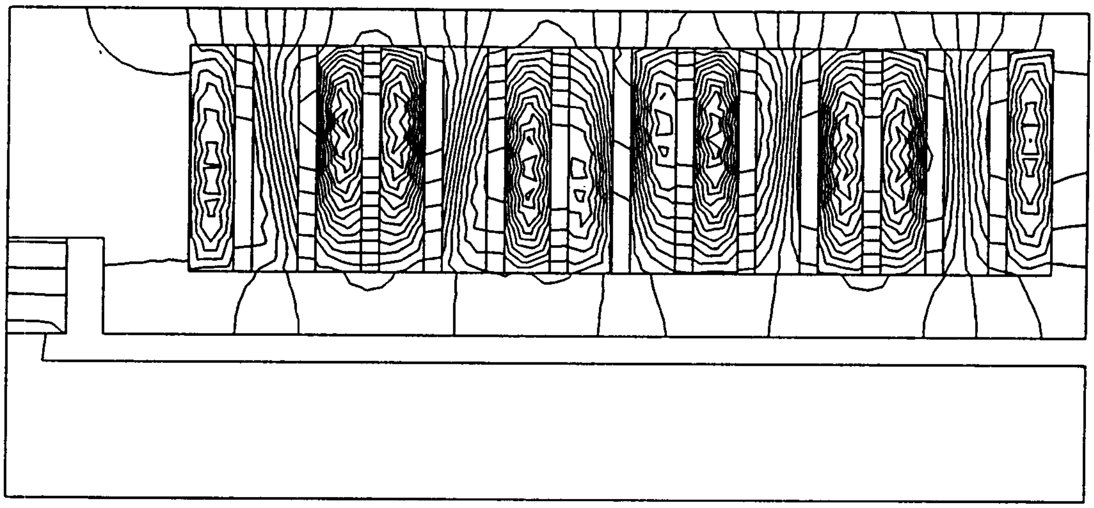

Fig. 4f Field lines of the fifth higher order mode, $f_R = 81.4$ MHz

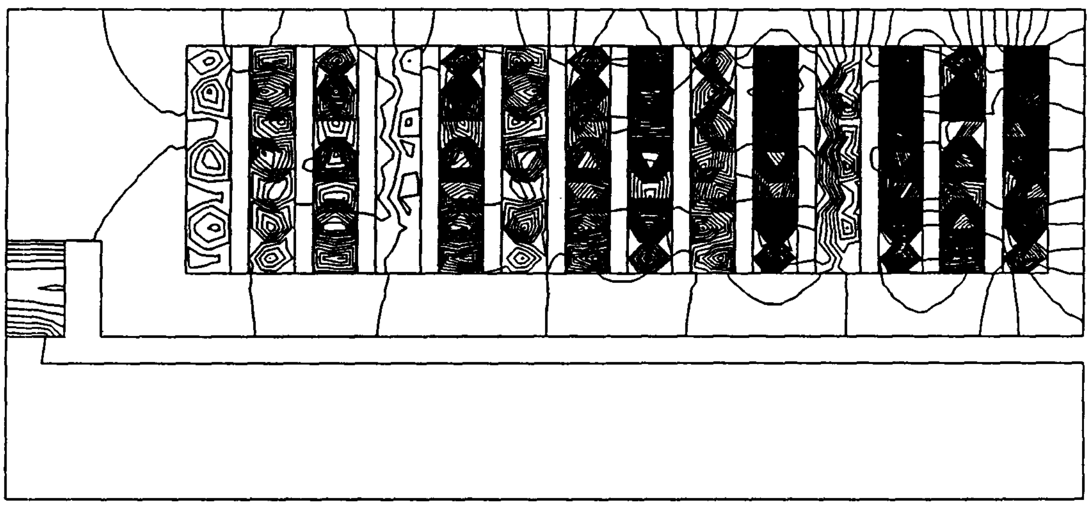

Fig. 4g Field lines of the 27^{th} higher order mode, $f_R = 309.8$ MHz

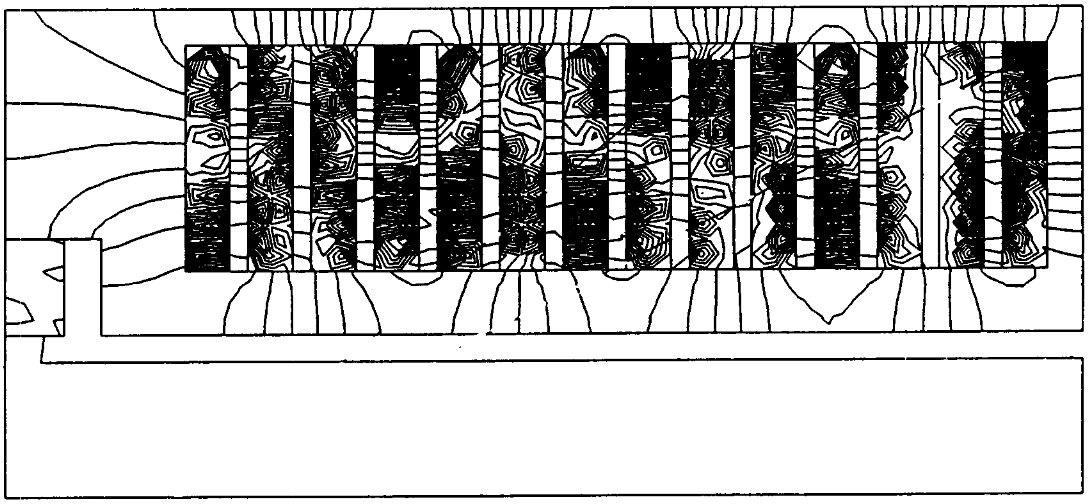

Fig. 4h Field lines of some higher order mode, $f_R = 724.6$ MHz